JOURNAL OF SOLID STATE CHEMISTRY 78, 46–51 (1989)

Comparative Study Based on Bond Competition Considerations of the Electronic Configuration of Nickel(III) in the K_2NiF_4-Type Oxides $Sr_{0.50}La_{1.50}Mg_{0.50}Ni_{0.50}O_4$ and $Sr_{1.50}La_{0.50}Ti_{0.50}Ni_{0.50}O_4$

ZHU LI MING, GÉRARD DEMAZEAU, MICHEL POUCHARD, JEAN MICHEL DANCE, AND PAUL HAGENMULLER

Laboratoire de Chimie du Solide du CNRS, Université de Bordeaux I, 351, cours de la Libération, 33405 Talence Cedex, France

Received November 9, 1987; in revised form August 10, 1988

Two new K_2NiF_4-type oxides $Sr_{0.50}La_{1.50}Ni_{0.50}Mg_{0.50}O_4$ and $Sr_{1.50}La_{0.50}Ti_{0.50}Ni_{0.50}O_4$ have been prepared. X-ray diffraction, magnetic measurements, and EPR investigations characterize a low-spin configuration in the octahedral sites of low spin Ni(III) ($t_{2g}^6e_g^1$). The nature of the distortion has been determined by comparing the $g_{//}$ and $g_\perp$ values at room temperature. While a strong elongation of the NiO_6 octahedra has been observed for $La_2Li_{0.50}Ni_{0.50}O_4$, quasi-regular octahedra can be expected for $Sr_{0.50}La_{1.50}Mg_{0.50}Ni_{0.50}O_4$ ($g_{//} \simeq g_\perp$) and compressed ones seem to occur in $Sr_{1.50}La_{0.50}Ti_{0.50}Ni_{0.50}O_4$ ($g_{//} > g_\perp$). An explanation of this structural evolution is proposed based on bond competition considerations.

Nickel(III) (d^7) can exhibit in an octahedral site two different electronic configurations: low-spin ($t_{2g}^6e_g^1$) and high-spin ($t_{2g}^5e_g^2$). Investigations on nickel(III) have been achieved for various oxide lattices, particularly those of perovskite and K_2NiF_4-type structure (*1–10*). Due to the large crystal field Ni(III) presents generally a low-spin configuration in such oxides. In $LaNiO_3$ thanks to strong covalency of the Ni(III)–O bonds the e_g electrons are delocalized (*11*) leading to metallic behavior. With decreasing rare-earth size ($LaNiO_3 \rightarrow LuNiO_3$) enhancement of the distortion of the perovskite structure leads to a weaker overlapping of the e_g orbitals of nickel and the p orbitals of oxygen. This phenomenon results in progressive localization of the e_g electron (*6*).

In a similar way in the $SrLnNiO_4$ (Ln = La, Nd, Sm, Eu, Gd) oxides with tetragonal K_2NiF_4-type structure, the two-dimensional character of the lattice and the strong covalency of the Ni(III)–O bonds lead to electronic delocalization in the perovskite layers and metallic behavior (*7*). Low-spin configuration appears in the isostructural $La_2Li_{0.50}Ni_{0.50}O_4$ oxide, but due to Li–Ni ordering the e_g electron is localized in the d_{z^2} orbital ($t_{2g}^6e_g^1$) including a Jahn–Teller-type elongation ($c_0/a_0 = 3.43$ (*10*)).

Weakening of the local crystal field in fluorides involving a low-spin → high-spin transition was observed for nickel(III) a few years ago (*12*). Such a transition has also been detected by EPR measurements for some oxides ($BaLaNiO_4$, $Sr_2NbIn_{0.90}Ni_{0.10}O_6$) where structure and composition favor the weaker crystal field of nickel(III) (*8*).

0022-4596/89 $3.00

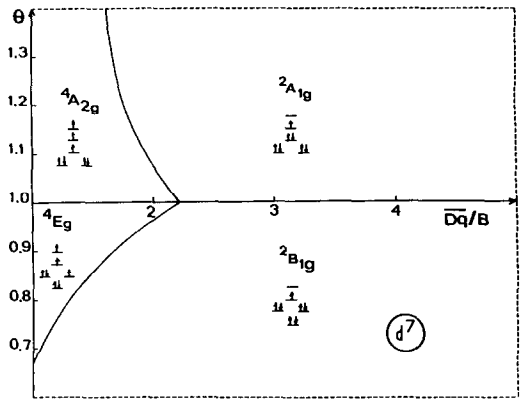

FIG. 1. Ground state domains for a d^7 configuration as a function of the structural distortion of the (MX_6) octahedron and the Dq/B ratio (Dq, average crystal field; B, Raccah parameter).

A simple model based on the magnitude of the crystal field and the energy values of the spectroscopic terms vs distortion of the MO_6 octahedra shows qualitatively the respective stability domains of the low- and high-spin configuration of a d^7 ion as a function either of elongation or of compression of the NiO_6 octahedra. In Fig. 1, θ represents the (Ni–O)Oz/(Ni–O)xOy ratio.

The K_2NiF_4-type layer structure of $(A,A')_2Ni_{0.50}M_{0.50}O_4$ oxides due to its 2D character is able to facilitate a structural distortion of the NiO_6 octahedron, but the distortion depends indeed on the competing chemical bonds.

In the xOy planes the same $2p$-oxygen orbitals are shared between the $(M–O)_{xOy}$ and $(Ni–O)_{xOy}$ bonds. On the other hand along the Oz axis the $(Ni–O)_{Oz}$ bond is also in competition with the (A,A')–O bonds. One may expect that a careful choice of the competing bonds $(M–O)_{xOy}$ and $(A',A)–O_{Oz}$ is able to influence strongly the distortion of the NiO_6 octahedra (Fig. 2).

Different combinations are possible: weak counterbonds in the xOy planes and strong (A,A')–O bonds favor, for instance, elongation of the NiO_6 octahedra (Fig. 2).

TABLE I

CALCULATED PAULING-TYPE IONICITY VALUES OF VARIOUS M–O BONDS (*12*)

M–O:	Sr–O	La–O	Li–O	Mg–O	Ti–O
Ionicities of Pauling	0.79	0.76	0.79	0.75	0.63

Such a behavior has been illustrated by the $La_2Li_{0.50}Ni_{0.50}O_4$ phase. In order to modify the NiO_6 distortion from an elongation to a compression it was indeed relevant to strengthen the covalent character of the competing $(M–O)$ bonds in the xOy plane and to weaken simultaneously the (A,A')–O bonds along the Oz axis.

To compare the influence of the ionicities of the various bonds involved we have chosen to investigate two new K_2NiF_4-type phases: $Sr_{0.50}Li_{1.50}Mg_{0.50}Ni_{0.50}O_4$ and $Sr_{1.50}La_{0.50}Ti_{0.50}Ni_{0.50}O_4$. Table I gives an order of magnitude of some bond ionicity values according to Pauling (*13*).

Preparation Methods

The $Sr_{0.50}La_{1.50}Mg_{0.50}Ni_{0.50}O_4$ phase was obtained in three steps. The first is a calci-

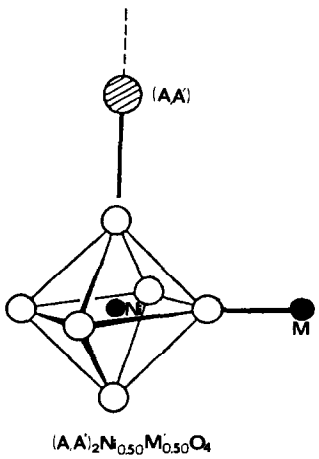

FIG. 2. Chemical bonding environment of the NiO_6 octahedron in the $(A,A')_2Ni_{0.50}M'_{0.50}O_4$ oxides with K_2NiF_4-type structure.

nation of a mixture of magnesium nickel and strontium nitrates with lanthanum acetate in stoichiometric proportions at 600°C. For preparing the analogous $Sr_{1.50}La_{0.50}Ti_{0.50}Ni_{0.50}O_4$ phase titanium was introduced as oxide (TiO_2) instead of nitrate. The second step is a thermal treatment (950°C) under oxygen flow for 48 hr. In order to stabilize oxidation state (III) of nickel the third step consists of a high oxygen pressure treatment (1.5 kbar) at high temperature (780°C) for 48 hr.

If some traces of starting oxides remain after the three treatments the resulting product is submitted again to the last oxidation reaction.

The oxidation state of nickel has been determined by chemical titration. For both phases the experimental value is 3.00 ± 0.03.

X-Ray Diffraction Study

The X-ray diffractograms of $Sr_{0.50}La_{1.50}Mg_{0.50}Ni_{0.50}O_4$ and $Sr_{1.50}La_{0.50}Ti_{0.50}Ni_{0.50}O_4$ characterize a tetragonal K_2NiF_4-type structure (space group *I4/mmm*). The K_2NiF_4 cell parameters (a_0, c_0) as well as c_0/a_0 are given in Table II. The value of c_0/a_0 decreases from $La_2Li_{0.50}Ni_{0.50}O_4$ to $Sr_{1.50}La_{0.50}Ti_{0.50}Ni_{0.50}O_4$.

For $Sr_{0.50}La_{1.50}Mg_{0.50}Ni_{0.50}O_4$ the existence of a weak line on the Guinier spectrum leads to indexation with a multiple cell ($a = a_0\sqrt{2}$, $c = c_0$). Such a superstructure suggests a 1 : 1 ordering in the xOy planes analogous to that observed in the previous $(A,A')_2Li_{0.50}M_{0.50}O_4$ phases (A = Ca, Sr, Ba; A' = La; M = Fe, Co, Ni) (*15*) or in the $ALaMg_{0.50}Fe_{0.50}O_4$ oxides (A = Ca, Sr, Ba) (*16*).

Surprisingly enough no extra X-ray line has been detected for $Sr_{1.50}La_{0.50}Ti_{0.50}Ni_{0.50}O_4$. As a rule cationic ordering in the perovskite layers of the K_2NiF_4 structure is favored both by charge and size differences. Whereas the formal charge difference is the same for the cationic couples Mg(II)–Ni(III) and Ti(IV)–Ni(III), the ionic radii according to Shannon and Prewitt (*17*) lead to a size difference between Mg(II) and Ni(III) (Δr = 0.17 Å) quite different from that of Ti(IV)–Ni(III) (Δr = 0.05 Å). Absence of Ti–Ni ordering can also be explained by the strong covalencies of both Ti–O and Ni–O bonds which attenuate actually the cation charge difference.

TABLE II

CRYSTALLOGRAPHIC PARAMETERS FOR SOME Ni(III) OXIDES WITH K_2NiF_4-TYPE STRUCTURE

	a	c_0	c_0/a_0
$La_2Li_{0.50}Ni_{0.50}O_4$ (*9*, *10*)	3.96	13.58	3.43
$Sr_{0.50}La_{1.50}Mg_{0.50}Ni_{0.50}O_4$	3.84	12.78	3.33
$Sr_{1.50}La_{0.50}Ti_{0.50}Ni_{0.50}O_4$	3.86	12.58	3.26
$SrLaAl_{0.98}Ni_{0.02}O_4$ (*14*)	3.86	12.98	3.36

Magnetic Study

The variation of the magnetic susceptibility vs temperature has been measured between 4.2 and 400 K using a Faraday-type balance. The thermal evolution of the reciprocal molar susceptibilities corrected from diamagnetic contributions for both nickel(III) phases are given in Figs. 3 and 4. For the $Sr_{0.50}La_{1.50}Mg_{0.50}Ni_{0.50}O_4$ phase the c_0/a_0 value (3.33) which is significantly weaker than that observed for $La_2Li_{0.50}Ni_{0.50}O_4$ (c_0/a_0 = 3.43) suggests a smaller elongation of the NiO_6 octahedron. If we assume that such a distortion is able to stabilize the low-spin state [i.e., the $^2A_{1g}$ (D_{4h}) ground term issued from the ^2E_g (O_h) term], a Van-Vleck corrective parameter $N\alpha$ must be introduced ($N\alpha = 2N\beta^2k^2/\Delta E$ for 0.5 Ni atoms (*18*)). Fitting of the experimental curve ($\chi'_M = C/T - \theta_p + N\alpha$) leads to a Curie constant $C_{Ni(III)} \simeq 0.51$ and an $N\alpha$ value ($N\alpha \simeq 140 \pm 10 \times 10^{-6}$ uem) much larger than that observed for the $La_2Li_{0.50}Ni_{0.50}O_4$ phase ($N\alpha \simeq 50 \times 10^{-6}$ uem). Variation of the anisot-

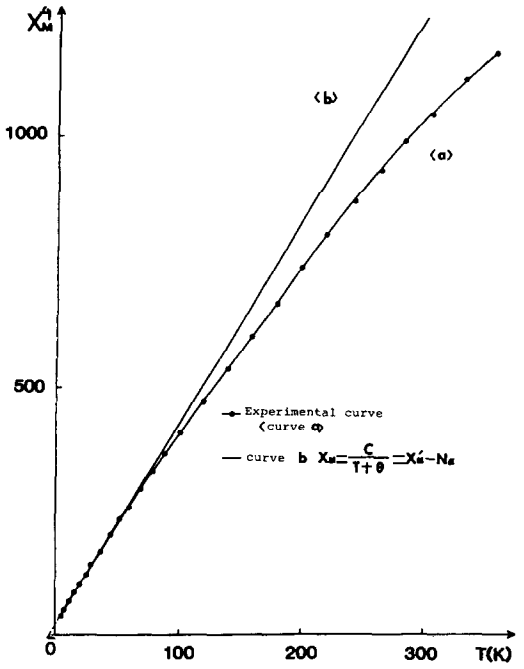

FIG. 3. Thermal evolution of the reciprocal molar susceptibility of $Sr_{0.50}La_{1.50}Mg_{0.50}Ni_{0.50}O_4$.

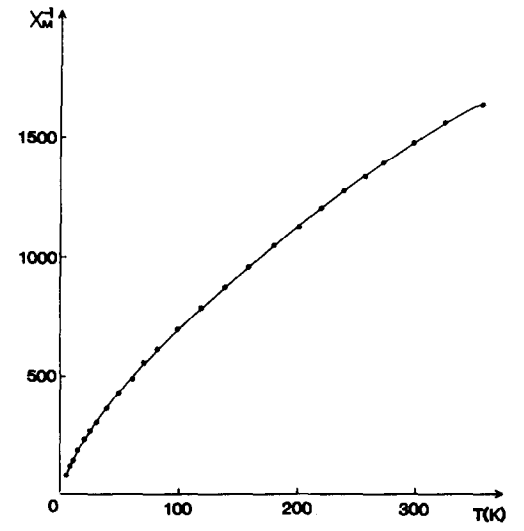

FIG. 4. Thermal evolution of the reciprocal molar susceptibility of $Sr_{1.50}La_{0.50}Ti_{0.50}Ni_{0.50}O_4$.

ropy of the $N\alpha$ term or presence of some high-spin Ni(III) at rising temperature should account for this discrepancy.

For the $Sr_{1.50}La_{0.50}Ti_{0.50}Ni_{0.50}O_4$ oxide the $\chi'^{-1}_M = f(T)$ curve is difficult to explain (Fig. 4). Such a nonlinear behavior could result from the absence of long-range Ti–Ni ordering in the perovskite planes with formation of Ni clusters or from a progressive low-spin → high-spin transition at rising temperature.

EPR Study

An EPR investigation was carried out to give more information about electronic structure and local distortion of the NiO_6 octahedra.

Figure 5 gives the EPR spectra of several K_2NiF_4-type phases: $La_2Li_{0.50}Ni_{0.50}O_4$, $Sr_{0.50}La_{1.50}Mg_{0.50}Ni_{0.50}O_4$, and $Sr_{1.50}La_{0.50}Ti_{0.50}Ni_{0.50}O_4$ at 300 K.

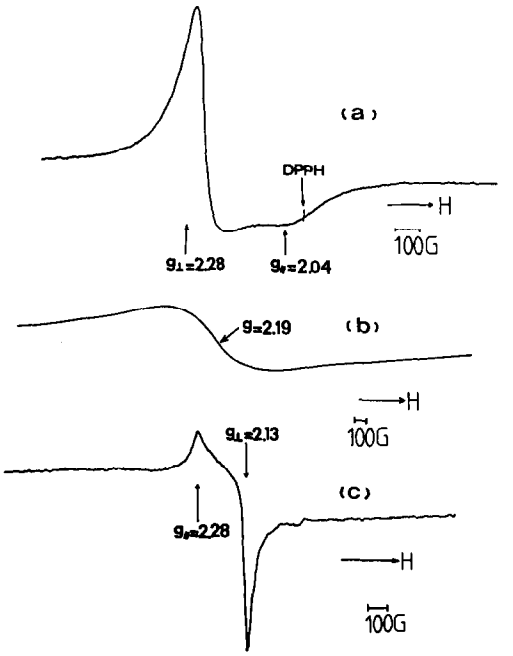

FIG. 5. EPR spectra at room temperature of (a) $La_2Li_{0.50}Ni_{0.50}O_4$, (b) $Sr_{0.50}La_{0.50}Mg_{0.50}Ni_{0.50}O_4$, and (c) $Sr_{1.50}La_{0.50}Ti_{0.50}Ni_{0.50}O_4$.

The measured g values are given in Table III, knowing that $g_{//}$ corresponds to a shoulder and $g_{\perp}$ to a derivative in the case of an axial tensor (*19*).

The EPR spectra of the $La_2Li_{0.50}Ni_{0.50}O_4$ and $Sr_{1.50}La_{0.50}Ti_{0.50}Ni_{0.50}O_4$ phases characterize an anisotropic electronic distribution ($g_{\perp} \neq g_{//}$). But if in the $La_2Li_{0.50}Ni_{0.50}O_4$ spectrum $g_{\perp} > g_{//}$, the opposite phenomenon, i.e., $g_{\perp} < g_{//}$, is observed for $Sr_{1.50}La_{0.50}Ti_{0.50}Ni_{0.50}O_4$.

On the contrary the EPR spectrum of the intermediate $Sr_{0.50}La_{1.50}Mg_{0.50}Ni_{0.50}O_4$ oxide shows only one isotropic peak ($g_{\perp} \simeq g_{//}$).

If we assume the existence of correlations between the local structural distortion and the respective g values, these EPR results can be interpreted in terms of evolution of the distortion of the NiO_6 octahedra.

TABLE III

EPR VALUES AT ROOM TEMPERATURE FOR Ni(III) OXIDES WITH THE K_2NiF_4-TYPE STRUCTURE

	$g_{//}$	$g_{\perp}$	g
$La_2Li_{0.50}Ni_{0.50}O_4$	2.04	2.28	2.20
$Sr_{0.50}La_{1.50}Mg_{0.50}Ni_{0.50}O_4$			2.19
$Sr_{1.50}La_{0.50}Ti_{0.50}Ni_{0.50}O_4$	2.28	2.13	2.18
$NaSrAl_{0.98}Ni_{0.05}O_4$ (4.2 K)	2.030	2.007	2.014

A strong NiO_6 elongation takes place in $La_2Li_{0.50}Ni_{0.50}O_4$ due to associated influence on the Ni–O bonds of the competing weak Li–O and strong La–O bonds (Fig. 6).

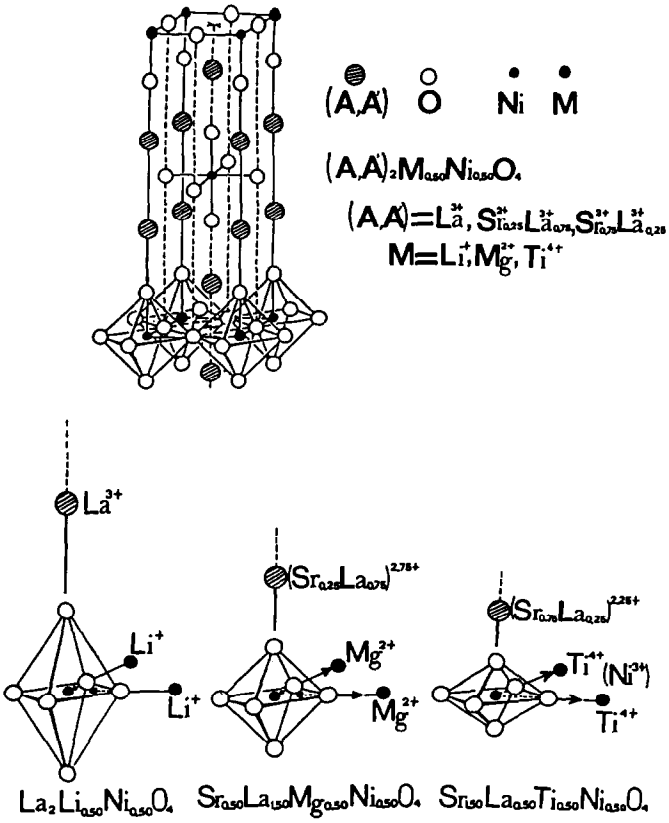

FIG. 6. Comparison of the distortions of the NiO_6 octahedron according to the nature of the chemical bonds in various Ni(III) oxides.

TABLE IV
PAULING'S IONICITY VALUES FOR THE (A)–O BONDS

A–O:	La–O	La–O	$Sr_{0.75}La_{0.25}$–O
Ionicities of Pauling	0.76	0.77	0.78

Absence of structural distortion (i.e., a pseudo-isotropic NiO_6 octahedron) should account for the one line spectrum observed for $Sr_{0.50}La_{1.50}Mg_{0.50}Ni_{0.50}O_4$. Qualitatively the weaker ionicity of the Mg–O bond compared to that of Li–O could explain the larger Ni–O distances in the xOy planes and disappearance of the NiO_6 elongation. Such an effect is enhanced by stronger ionicity of the $(Sr_{0.25}La_{0.75})$–O bonds along the Oz axis compared to that of the La–O bonds (Fig. 6). Conjunction of both phenomena may logically account for the isotropy of the NiO_6 octahedra.

Replacing the Mg–O bond by a much more covalent Ti–O bond in the perovskite layers and increasing the ionicity of the competitive (A,A')–O bond [here a $(Sr_{0.75}La_{0.25})$–O bond (see also Table IV)] along the c axis could allow us in a similar way to obtain squeezed NiO_6 octahedra in $Sr_{1.50}La_{0.50}Ti_{0.50}Ni_{0.50}O_4$ ($g_\perp < g_\parallel$) (Fig. 6). P. Ganguly has stressed a similar phenomenon in $SrNdAl_{0.98}Ni_{0.02}O_4$ with a similar K_2NiF_4-type structure ($g_\parallel = 2.03$, $g_\perp = 2.007$ at 4.2 K) (*14*).

Such an interpretation of the evolution of the structural distortion of the NiO_6 octahedra in these three oxides with K_2NiF_4-type structure is strongly supported by the decrease of the c_0/a_0 values from 3.43 ($La_2Li_{0.50}Ni_{0.50}O_4$) to 3.26 ($Sr_{1.50}La_{0.50}Ti_{0.50}Ni_{0.50}O_4$). An EXAFS study is in progress in order to determine the exact Ni–O distances.

Absences in the recorded EPR spectra of a g value close to 4 seems to exclude, at least at 300 K, occurrence of high-spin Ni(III) in the three investigated oxides. Figure 6 summarizes clearly the conclusions of our comparative study.

References

1. L. D. BYER, B. S. BORIE, AND G. PEDRO SMITH, *J. Am. Chem. Soc.* **76,** 1499 (1954).
2. B. L. CHAMBERLAND AND W. H. CLOUD, *J. Appl. Phys.* **40,** 434 (1969).
3. A. WOLD, E. POST, AND E. BANKS, *J. Amer. Chem. Soc.* **79,** 4911 (1957).
4. W. C. KOEHLER AND I. O. WOLLAN, *J. Phys. Chem. Solids* **2,** 100 (1957).
5. J. B. GOODENOUGH AND P. M. RACCAH, *J. Appl. Phys. B* **6,** 1031 (1965).
6. G. DEMAZEAU, A. MARBEUF, M. POUCHARD, AND P. HAGENMULLER, *J. Solid State Chem.* **3,** 582 (1971).
7. G. DEMAZEAU, M. POUCHARD, AND P. HAGENMULLER, *J. Solid State Chem.* **18,** 159 (1976).
8. G. DEMAZEAU, J. L. MARTY, B. BUFFAT, J. M. DANCE, M. POUCHARD, P. DORDOR, AND B. CHEVALIER, *Mater. Res. Bull.* **17,** 37 (1982).
9. G. BLASSE, *J. Inorg. Chem.* **27,** 2683 (1965).
10. G. DEMAZEAU, J. L. MARTY, M. POUCHARD, T. ROJO, J. M. DANCE, AND P. HAGENMULLER, *Mater. Res. Bull.* **16,** 47 (1981).
11. J. B. GOODENOUGH, "Magnetism and the Chemical Bond," Wiley–Interscience, New York (1961).
12. J. GRANNEC, J. PORTIER, M. POUCHARD, AND P. HAGENMULLER, *J. Inorg. Nucl. Chem.* **11** (Suppl.) (1976).
13. L. PAULING, "The Nature of the Chemical Bond," 3rd ed., Cornell Univ. Press, Ithaca, NY (1960).
14. P. GANGULY, Thèse d'Université, Bordeaux I (1984).
15. G. DEMAZEAU, B. BUFFAT, M. POUCHARD, AND P. HAGENMULLER, *J. Solid State Chem.* **54,** 389 (1984).
16. G. DEMAZEAU, ZHU LI MING, L. FOURNES, M. POUCHARD, AND P. HAGENMULLER, *J. Solid State Chem.* **72,** 31 (1988).
17. R. D. SHANNON AND C. T. PREWITT, *Acta Crystallogr. Sect. B* **25,** 925 (1969).
18. B. N. FIGGIS, "Introduction to Ligand Field," Wiley–Interscience, New York (1963).
19. R. LACROIS, C. HÖCHLI, AND K. A. MÜLLER, *Helv. Phys. Acta* **37,** 627 (1964).